



Garza, C., Das, R., Shterenlikht, A., & Pavier, M. (2017).  
Measurement of assembly stress in composite structures using the  
deep-hole drilling technique. *Composite Structures*.  
<https://doi.org/10.1016/j.compstruct.2017.12.031>

Peer reviewed version

Link to published version (if available):  
[10.1016/j.compstruct.2017.12.031](https://doi.org/10.1016/j.compstruct.2017.12.031)

[Link to publication record in Explore Bristol Research](#)  
PDF-document

This is the author accepted manuscript (AAM). The final published version (version of record) is available online via Elsevier at <https://www.sciencedirect.com/science/article/pii/S026382231733698X?via%3Dihub>. Please refer to any applicable terms of use of the publisher.

## University of Bristol - Explore Bristol Research

### General rights

This document is made available in accordance with publisher policies. Please cite only the published version using the reference above. Full terms of use are available:  
<http://www.bristol.ac.uk/red/research-policy/pure/user-guides/ebr-terms/>

# MEASUREMENT OF ASSEMBLY STRESS IN COMPOSITE STRUCTURES USING THE DEEP-HOLE DRILLING TECHNIQUE

Carlos Garza<sup>1</sup>, Raj Das<sup>2</sup>, Anton Shterenlikht<sup>3</sup>, Martyn Pavier<sup>3</sup>

*<sup>1</sup>Consejo Nacional de Ciencia y Tecnología, Av. Insurgentes Sur 1582, Col. Crédito Constructor, 03940, Mexico City, Mexico*

*<sup>2</sup>Sir Lawrence Wackett Aerospace Research Centre, School of Engineering, RMIT University, GPO Box 2476, Melbourne, Victoria 3001, Australia*

*<sup>3</sup>Department of Mechanical Engineering, University of Bristol, Queen's Building, University Walk, Bristol, BS8 1TR, United Kingdom*

*Corresponding Author: Martyn Pavier, E-Mail: [martyn.pavier@bristol.ac.uk](mailto:martyn.pavier@bristol.ac.uk), Tel.: +44 7766 463 299*

## Abstract

The deep-hole drilling (DHD) method is a residual stress measurement method that is widely used for measurements in thick metallic components. In the DHD method a reference hole is first drilled through the thickness of the component. The diameter of the hole is measured accurately and then a cylindrical core of material around the hole is trepanned from the component, relaxing the residual stresses in the core. Finally, the diameter of the reference hole is re-measured and the change in diameter used to calculate the residual stress. In this work the method is used to attempt the measurement of cure and assembly stress in thick AS4/8552 composite laminates. The results indicate that although the DHD method cannot measure cure stress, it is able to measure assembly stress. Furthermore, a modification to the standard DHD method allows the through-thickness component of assembly stress to be measured in angle components.

**Keywords:** residual stress; assembly stress; deep hole drilling; composite structures

## 1 INTRODUCTION

The latest generation of civil aircraft use carbon fibre composite components throughout their structure. Some of these components have very large sections, sometimes up to 50 mm or more in thickness. Typical examples are wing skins and landing gear attachment ribs. For such components, residual stresses introduced during the manufacturing process will exist and require quantification to ensure safe and economic operation. A major cause of residual stress in a composite structure is assembly stress. Figure 1 shows a schematic diagram of the assembly of a wing box from two spars and two wing skins. Distortion of the wing spars during manufacture [1,2] leads to a mis-fit between the components and results in an assembly stress in the final structure. Current practice is to minimise the level of assembly stress by the use of shims [3, 4], but this is an expensive and time-consuming procedure.

Of particular concern is the generation of a through-thickness component of assembly stress in the corners of components such as wing spars. In Figure 1 the flanges of the spars are bent inwards during assembly, giving rise to a compressive through-thickness stress. If instead the flanges were bent outwards, a tensile through-thickness stress would develop, leading to an increased likelihood of delamination [5].

The problem of measuring the residual stress in composite materials has attracted previous attention, although many techniques that have been attempted are not suitable for measurements in thick sections. Schajer and Yang [6] used the hole-drilling method used to measure residual stress in isotropic materials and modified the analysis so that it could be applied to composite materials. In the hole-drilling method a strain gauge rosette is bonded to the surface of the laminate and then a hole is drilled through the centre of the rosette. The residual stress is calculated from the strain changes measured by the rosette. Sicot et al. [7] describe an incremental hole-drilling method to measure residual stress in a 1 mm thick carbon/epoxy laminate. Incremental hole-drilling method is an extension to the original hole-drilling method allowing the variation of residual stress with depth to be measured. More recently, the hole-drilling method has been combined with a moiré technique [8], digital image correlation (DIC) [9-11] and electronic speckle-pattern interferometry [12] to improve the accuracy of the method.

Raman microscopy was used by Filiou and Galiotis [13] to measure the residual strain in individual fibres in carbon-fibre thermoplastic composite. This work is however concerned

with what Barnes and Byerly [14] term ‘microstresses’: microscopic residual stress arising from the difference in thermal properties of the fibre and resin.

Guemes and Menéndez [15] used Bragg grating fibre-optic sensors embedded in a 7 mm thick carbon/epoxy quasi-isotropic laminate. A hole was drilled close to the point of intersection of the fibres. Results showed that stresses of the order of 50 MPa were released by the hole drilling. Although suitable for measuring residual stress in the plane of the composite, the technique would be difficult to use to measure residual stresses between plies.

Cowley and Beaumont [16] describe a layer removal technique to measure the residual stress by machining away near surface plies and then measuring the resulting curvature of the remaining laminate. Ersoy and Vardar [17] also used a layer removal technique, except that they removed layers by forcing a knife blade between plies. Such techniques are unsuitable for thick section components because the resulting curvature is so small.

In addition to experimental work to measure the residual stress in composites, attempts have been made to predict the residual stress from theoretical models of the manufacturing process. Bogetti and Gillespie [18] used a method based on laminate theory to predict residual stresses arising from shrinkage of the resin during cure and mismatch of thermal expansion coefficients between plies. Other work has used the finite element method to predict residual stress [19]. Such analyses are not straightforward and do not provide reliable predictions of residual stress because the necessary thermal and mechanical properties of the resin are difficult to measure and change during cure.

In this paper, the use of the deep-hole drilling (DHD) method is used to measure the assembly stress in thick section composites. The DHD method is a well-established residual stress measurement method for metallic materials and is particularly suitable for large, thick section components. Initial development of the deep-hole method was carried out by Zhadanov and Gonchar [20], Beaney [21], and Jesensky and Vargova [22]. More recent improvements to the deep-hole method have been made by Smith and his co-workers [23-27]. An attempt has been made to use the DHD method to measure the cure residual stresses in a thick section composite laminate [28] but we will show here that such a measurement leads to substantial error.

## 2 DEEP-HOLE METHOD FOR ORTHOTROPIC MATERIALS

In the DHD method, a hole is first drilled through the thickness of the component using a gun drill (Step 1 of Figure 2). Next the diameter of the hole is measured accurately using an air probe (Step 2 of Figure 2) and then a cylindrical core of material around the hole is trepanned from the component, relaxing the residual stresses in the core (Step 3 of Figure 2). For metallic components an electro-discharge machining method (EDM) can be used to trepan the core but for composite materials a diamond tipped hole saw has been found to be suitable. Finally, the diameter of the hole is re-measured and the change in diameter used to calculate the residual stress (Step 4 of Figure 2). The DHD method assumes that the relaxation of residual stress at the trepan radius caused by the introduction of the reference hole is negligible and that the residual stresses are completely relaxed in the trepanned core in a linear elastic manner. Figure 2 also shows the front and back bushes that are adhesively bonded to the component to provide a residual stress free datum.

Figure 3(a) shows a cross section through the thickness of a component being measured. The air probe measures the diameter  $d_0$  before trepanning and the diameter  $d$  after trepanning. Depending on the variation of residual stress with depth, the diameter  $d$  will vary through the thickness of the component. Figure 3(b) shows a cross section of the hole measured at one depth. In general the circular hole will distort into an elliptic hole so that the diameter varies with the angular position  $\theta$ .

The calculation of the residual stress from the change in diameter of the hole requires the evaluation of a set of coefficients based on an analysis of the distortion of a hole in a plate loaded by far-field direct and shear stresses. For isotropic materials the evaluation uses the Mitchell solution for the elastic deformation of a hole in a plate [29]. For orthotropic materials the coefficients can be derived from Lekhnitskii's analysis [30, 31].

The coefficients used in the DHD calculations of residual stress,  $f_\theta$ ,  $g_\theta$  and  $h_\theta$ , are defined by

$$\frac{u_r}{a} = \frac{d(\theta) - d_0}{d_0} = \frac{1}{E_1} (f_\theta \sigma_{11}^0 + g_\theta \sigma_{22}^0 + h_\theta \sigma_{12}^0) \quad (1)$$

where  $u_r$  is the radial displacement at the hole edge at angle  $\theta$  to the major principal material direction,  $a$  is the radius of the hole and  $\sigma_{11}^0$ ,  $\sigma_{22}^0$  and  $\sigma_{12}^0$  are far-field applied stresses in the principal material coordinate system. Figure 4 shows the global  $xy$  coordinate system used for the measurement and the principal material coordinate system. The angle  $\varphi = \theta + \alpha$  is the angle between the global  $x$  axis and the angular position of the measurement of radial displacement where  $\alpha$  is the angle between the fibre direction and the  $x$  axis.

The coefficients  $f_\theta$ ,  $g_\theta$  and  $h_\theta$  are dimensionless functions of  $\theta$  that depend on the orthotropic material constants.

$$f_\theta = \frac{1}{2} [1 + n - k + (1 + n + k) \cos 2\theta] \quad (2)$$

where

$$k = \sqrt{\frac{E_1}{E_2}}, \quad n = \sqrt{2(k - \nu_{12}) + \frac{E_1}{G_{12}}} \quad (3)$$

$$g_\theta = \frac{1}{2} [k^2 + nk - k - (k^2 + nk + k) \cos 2\theta] \quad (4)$$

and

$$h_\theta = \frac{1}{2} (n^2 + nk + n) \sin 2\theta \quad (5)$$

In Eq. (1) to Eq. (5),  $E_1$ ,  $E_2$  are the Young's moduli of the material in the major and minor principal material directions,  $\nu_{12}$  is Poisson's ratio for loading in the major principal material direction and  $G_{12}$  the shear modulus.

Finite element analysis has been carried out using Abaqus 6.12 to provide validation of these equations [31]. The material properties used for these analysis are for unidirectional carbon/epoxy AS4/8552 as defined in Table 1, giving  $k = 3.75$  and  $n = 5.733$ . Figure 5 shows a comparison of the values of the coefficients obtained from finite element analysis with those

evaluated using Eqs. (2), (4) and (5). In Figure 5, the coefficients  $g_\theta$  and  $h_\theta$  have been divided by  $k$  so that the range of values for all coefficients are similar.

### 3 MEASUREMENT OF CURE STRESS

In previous work carried out by some of the authors, an attempt was made to measure the cure stress in a composite laminate using the DHD method [28]. Two measurements were made of the cure stress in a 22mm thick composite plate produced by resin film infusion. The finite element method was used to calculate the coefficients used in the method to relate the measured hole distortion to the residual stress. In this section of the paper we shall demonstrate that the DHD method cannot be used to measure accurately the cure stress, unless the hole diameter and trepan diameter are much smaller than the thickness of blocks of plies of the same orientation. In practice, with current technology, this is unachievable.

To investigate the ability of the DHD to measure cure stress, a 160 mm by 80 mm laminated plate was fabricated of AS4/8552 carbon/epoxy prepreg with a thickness of 18 mm thickness. The laminate contained 10 blocks of plies, each formed of 16 prepreg plies with the same orientation, giving the lay-up sequence in standard notation of  $[0_{16}, -45_{16}, +45_{16}, 90_{16}, 0_{16}]_s$ . The block size, that is the total thickness of similarly orientated plies, for the laminate was 1.8 mm. The AS4/8552 laminate was cured in an autoclave using the recommended cure cycle for thick specimens [32].

After cure, aluminium front and back bushes were bonded to the laminate. A 3 mm diameter measurement hole was then drilled using a gun drill, followed by a 10 mm inside diameter diamond tipped hole saw [33] to trepan away the material around the hole.

A finite element model of the laminate was created using Abaqus 6.12 as shown in Figure 6 with 20 noded quadratic brick elements (Abaqus element type C3D20). The numbers in the figure give the number of elements along the sides of the model. The large number of elements through the thickness of the model were used to give an accurate prediction of the change in diameter of the measurement hole during a simulation of the DHD method.

To simulate the DHD measurement of cure stress, a thermal cool-down step was first carried out using the thermal expansion coefficients for AS4/8552 defined in Table 1 and a change of temperature  $\Delta T$  of  $-160^\circ\text{C}$ . This produced the square section fibre direction stress profile

through the thickness of the laminate shown in Figure 7 by the solid line. Note the fibre direction stresses do not sum to zero, although the stresses in the global directions do.

Next, the DHD method was simulated by removing elements along the axis of the hole using the technique of element removal to simulate drilling of the measurement hole, followed by removing the elements forming a hollow cylinder around the axis of the hole to simulate the trepanning step. The change in diameter of the hole after trepanning was used to simulate the measurement of residual stress using Eq. (1). The results of the DHD simulation are shown in Figure 7 by the dashed lines. For the simulation, two different sizes of hole and drepan diameter were used. The large hole simulation shown in Figure 7 used a hole diameter of 3 mm and a core diameter of 8 mm while the small hole simulation used a hole diameter of 0.5 mm and a core diameter of 1 mm. The large hole dimeters match those used in the experimental measurement. The large hole simulation results show no agreement with the original predicted residual stress profile while the small hole simulation results show good agreement, but only in the centre of each block of plies. Figure 7 also shows the experimental measurements obtained using the DHD procedure. The experimental measurements show a good agreement with the results of the FE simulation using the large hole diameter, but no agreement with the cure stress profile predicted by FE.

The results of this study indiate that for an accurate measurement of cure stress, the hole and trepan diameters must be small compared to the block size. Current practice is to use thin blocks of plies [34], in which case a DHD measurement of cure stress using existing technology is impossible.

## **5 MEASUREMENT OF IN-PLANE ASSEMBLY STRESS**

The schematic diagram of the generation of assembly stress in Figure 1 shows the two wing skins are subjected to bending after assembly. A study was therefore carried out to determine whether the DHD method is able to measure a bending stress in a composte specimen. A pair of beam specimens of 20 mm width were cut from a plate with the same lay-up sequence defined in the previous section, so that the  $0^\circ$  direction is along the beam. These specimen were loaded in a 4-point bend rig using a strain gauge orientated along the beam attached to the upper surface of the specimen to measure the level of bending, as shown in Figure 8.

Each specimen was loaded until the strain gauge measured the desired strain, whereupon the



gauge was removed and front and back bushes for DHD stress measurement were bonded to the specimen. One specimen was loaded to a strain of 700  $\mu\epsilon$  and the other to a strain of 1400  $\mu\epsilon$ . In this paper we will only present the results for the most heavily loaded beam, but a full set of results are available elsewhere [35]. The DHD procedure was carried out as described in previous sections, except that the hole saw was not used to trepan through the final 0° block of plies in case the core broke away from the back bush.

A simulation of the DHD measurement was carried out using FEA, as described in the previous section. The FE mesh that was used is shown in Figure 9. 20 noded quadratic brick elements (Abaqus element type C3D20) were used as before. Again, the numbers in the figure give the number of elements along the sides of the model. A thermal cool down step was carried out before the bending load was applied. Sufficient bending load was applied so that the strain on the surface of the beam matched the strain measured by the gauge in the experiment. The simulation of the DHD measurement used a hole diameter of 3 mm and a core diameter of 10 mm to match that used in the experiment.

The results of the experimental measurement and FE simulation are shown in Figure 10. Only the fibre direction stresses are shown. The experimental measurements show an acceptable agreement with the results of the FE simulation, except near the bottom surface of the specimen. This is because the hole saw did not trepan through the final block of plies. The FE simulation of the measurement did not match precisely the originally predicted residual stress since the residual stress contained the cure stress in addition to the bending stress. The difference in stress between the two sets of results is of the order of 50 MPa, similar to the magnitude of the cure stress.

## **5 MEASUREMENT OF THROUGH-THICKNESS ASSEMBLY STRESS**

In Figure 1 showing the generation of assembly stress by the fabrication of structure from a number of slightly distorted components, a through-thickness component of assembly stress will be generated in the corners of the angle components. By through-thickness component we mean the component of direct stress in the direction normal to the surface of the component. When fabrication causes the angle to reduce, a through-thickness compressive stress will be generated and when the angle increases, tensile stress will be generated. [2] Magnitudes of tensile through-thickness residual stress of the order of 20 MPa would be a concern since the strength of the laminate is low in this direction.

Right angle specimens were manufactured by autoclave from AS4/8552 prepreg plies using a curved invar female tool and with a lay-up sequence of  $[(0, +45, -45, 90)_7]_s$  to the dimensions shown in Figure 11 [36]. Loading caps were attached to the ends of the angle specimen so that a bending moment could be applied to by compressing the assembly of specimen and loading caps between the platens of a test machine. The dimensions of the loading caps are shown in Figure 11 and Figure 12 shows the assembly located in the test machine. Three specimens were tested in this work. One specimen was tested without any applied load. For the other two specimens, one had a compressive load of 1 kN applied, the other 1.5 kN. Once the specimens had been loaded, the turnbuckle shown in Figure 12 was tightened so that the assembly could be removed from the test machine. DHD bushes were then attached to the specimen.

The method of measuring the through-thickness assembly stress can be seen in Figure 13. The same general method was used in previous work to measure the through thickness stress in a quenched steel specimen [37]. A reference hole of 3 mm diameter was drilled through the corner of the specimen to take the actuation rod of a TESA SA GTL21 LVDT. One end of the rod was attached to the outer bush, the other end to the LVDT itself. The same hole saw used for earlier work was then used to trepan material from around the reference hole, as shown in Figure 13. Trepanning was carried out in increments of 1 mm through the thickness of the angle specimen. After each increment, any rise in temperature due to the trepanning was allowed to dissipate and the axial distortion of the core was then measured.

As previously, a simulation of the DHD measurement was carried out using FEA using the mesh shown in Figure 14 constructed of 20 noded quadratic brick elements. A thermal cool down step was carried out before the bending load was applied. Bending load of 1.5 kN was applied to the model to match that used for the most heavily loaded experimental specimen. Simulation of the trepanning was then carried out in increments of 1 mm to produce the results shown in Figure 15. A quartic was fitted to the data using a least-squares algorithm to produce the solid curve in Figure 15. A quartic was chosen so that the rate of change of length with trepan depth could be made zero at both surfaces so as to match the condition there of zero through thickness stress. The quartic was then differentiated with respect to trepan depth and multiplied by the through thickness Young's modulus  $E_3$  (Table 1) to give the through-thickness stress profile in Figure 16. This profile is compared with the original profile predicted by FEA with good agreement. Note that some error is introduced because of the

curvature of the specimen and therefore the trepan does not remove a uniform thickness of material near the surfaces.

The experimentally measured change of core length with depth for the three specimens is shown in Figure 17. Due to the variability of the experimental data, no attempt was made to fit a quartic and instead a least-squares linear fit was used, as seen in the figure. The slope of the lines multiplied by the through-thickness Young's modulus gives a measurement of the average through-thickness stress. The results are shown in Table 2, compared with the maximum stress obtained from the FEA predicted and simulated profile with reasonable agreement. Some error is introduced in both the FE simulation and the experimental measurement since trepanning relaxes both the through-thickness and the in-plane stress and both effect the change in length of the core.

## **6 CONCLUSIONS**

In this work, the ability of the DHD method to measure cure stress and assembly stress in a thick composite laminate has been assessed. FEA has been used to predict the magnitude of cure stress and assembly stress, and has also been used to simulate the DHD procedure to determine in principle the ability of the procedure to make accurate measurements.

It has been shown that the DHD method is unable to measure the cure stress unless the thickness of blocks of similarly orientated plies is larger than the hole size used in the DHD procedure. Current practice is to use thin blocks, in which case DHD cannot be used to measure the cure stress.

DHD measurements of assembly stress have been shown to be in acceptable agreement with the stress predicted by FEA. This acceptable agreement has been obtained both for the measurement of in-plane assembly stress and the through-thickness assembly stress in the corner of specimens with an angle geometry.

## **ACKNOWLEDGEMENTS**

The authors would like to acknowledge Steve Harding, University of Bristol and Xavier Ficquet, VEQTER Ltd. for providing technical support for the experimental studies. The angle specimens used in the work were provided by the Advanced Composites Centre for Innovation and Science (ACCIS) at the University of Bristol. The financial support from the Mexican

National Council for Science and Technology (CONACyT), the Institute of Innovation and Technology Transfer (I<sup>2</sup>T<sup>2</sup>) and the Government of Nuevo León is gratefully acknowledged.

## REFERENCES

1. Kappel E, Stefaniak D and Hühne C, Process distortions in prepreg manufacturing – An experimental study on CFRP L-profiles, *Composite Structures*, 106, 615-625, 2013
2. Kappel E, Stefaniak D and Fernlund G, Predicting process-induced distortions in composite manufacturing – A pheno-numerical simulation strategy, *Composite Structures*, 120, 98-106, 2015
3. Söderberg R, Wärmefjord K and Lindkvist L, Variation simulation of stress during assembly of composite parts, *CIRP Annals- Manufacturing Technology* 64, 17-20, 2015
4. Liu, L. The influence of the substrate's stiffness on the liquid shim effect in composite-to-titanium hybrid bolted joints. *Proc IMechE Part G: J. Aerospace Engineering*, 228, 470-479, 2014
5. Feih S and Shercliff HR, Composite failure prediction of single-L joint structures under bending. *Composites Part A*, 36, 381-395, 2005
6. Schajer GS and Yang L, Residual-stress measurement in orthotropic materials using the hole-drilling method, *Experimental Mechanics*, 34, 324-333, 1994
7. Sicot O, Gong XL, Cherouat A and Lu J, Determination of residual stress in composite laminates using the incremental hole-drilling method, *Journal of Composite Materials*, 37, 831-844, 2003
8. Chai GB, Chin HK, Xie H and Asundi A, Residual interlaminar deformation analysis in the carbon/epoxy composites using micro-moiré interferometry, *Composites Science and Technology*, 63, 171-175, 2003
9. Baldi, A. Full field methods and residual stress analysis in orthotropic material. I: Linear approach, *Int. J. Solids Structures*, 44, 8229-8243, 2007
10. Baldi, A. Full field methods and residual stress analysis in orthotropic material. II: Nonlinear approach, *Int. J. Solids Structures*, 44, 8244-8258, 2007
11. Baldi, A. Residual stress analysis of orthotropic materials using integrated digital image correlation, *Experimental Mechanics*, 54, 1279-1292, 2014

12. Pisarev, VS, Eleonsky, SI, Chernov, AV. Residual stress determination in orthotropic composites by displacement measurements near through hole, *Experimental Mechanics*, 55, 1225-1238, 2015
13. Filiou C and Galiotis C, In situ monitoring of the fibre strain distribution in carbon-fibre thermoplastic composites: 1. Application of a tensile stress field, *Composites Science and Technology*, 59, 2149-2161, 1999
14. Barnes JA and Byerly GE, The formation of residual stresses in laminated thermoplastic composites, *Composites Science and Technology*, 51, 479-494, 1994
15. Guemes JA and Menéndez JM, Response of Bragg grating fiber-optic sensors when embedded in composite laminates, *Composites Science and Technology*, 62, 959-966, 2002
16. Cowley KD and Beaumont PWR, The measurement and prediction of residual stresses in carbon-fibre/polymer composites, *Composites Science and Technology*, 57, 1445-1455, 1997
17. Ersoy N and Vardar Ö, Measurement of residual stresses in layered composites by compliance method, *Journal of Composite Materials*, 34, 575-598, 2000
18. Bogetti TA and Gillespie Jr. JW, Process-induced stress and deformation in thick-section thermoset composite laminates, *Journal of Composite Materials*, 26, 626-660, 1992
19. Jounston A, Vaziri R and Poursartip A, A plane strain model for process-induced deformation of composite structures, *Journal of Composite Materials*, 35, 1435-1469, 2001
20. Zhandanov IM and Gonchar AK, Determining the residual welding stresses at depth in metals, *Automatic Welding*, 1978, Vol. 31, 22-24
21. Beaney EM, Measurement of sub-surface stress, CEGB Report Rd/B/N4325, 1978
22. Jesensky M and Vargova J, Calculation and measurement of stresses in thick-walled pressure vessels, *Svaracske Spravy*, 4, 79-87, 1981
23. Leggatt RH, Smith DJ, Smith SD and Faure F, Development and experimental validation of the deep-hole method for residual stress measurements, *Journal of Strain Analysis*, 31, 177-186, 1996
24. Bonner NW and Smith DJ, Measurement of residual stresses using the deep-hole method, *Pressure Vessels and Piping*, 327, 53-65, 1996

25. Smith DJ, Bouchard PJ and George D, Measurement and prediction of through thickness residual stresses in thick section welds, *Journal of Strain Analysis*, 35, 287-305, 2000
26. George D, Kingston E and Smith DJ, Measurement of through-thickness stresses using small holes, *Journal of Strain Analysis*, 37, 125-139, 2002
27. Wimpory RC, May PS, O'Dowd NP, Webster GA, Smith DJ and Kingston E, Measurement of residual stresses in T-plate weldments, *Journal of Strain Analysis*, 38, 349-365, 2003
28. Bateman MG, Miller OH, Palmer TJ, Breen CEP, Kingston EJ, Smith DJ, Pavier MJ. Measurement of residual stress in thick section composite laminates using the deep-hole method. *International Journal of Mechanical Sciences*, 47, 1718–1739, 2005.
29. Timoshenko S and Goodier JN, *Theory of Elasticity*, 1951, McGraw Hill
30. Lekhnitskii SG, *Anisotropic Plates*, 1968. Gordon and Breach
31. Garza, C, Shterenlikht, A, Pavier, MJ, Smith, DJ. Exact solutions of hole distortion for use in deep hole drilling measurements of residual stress in orthotropic plates, *Journal of Strain Analysis*, 52, 77-82, 2016
32. Oh JH and Lee DG, Cure cycle for thick glass/epoxy composite laminates, *Journal of Composite Materials*, 36, 19–45, 2002
33. Industrial Abrasives Ltd, PO Box 1101, Bournemouth, BH8 9YR, UK
34. Fuller, JD, Wisnom, MR. Pseudo-ductility and damage suppression in thin CFRP angle-ply laminates, *Composites Part A*, 69, 64-71, 2015
35. Garza Rodriguez C, Deep-hole drilling measurements of residual and assembly stress in composite materials, PhD thesis, University of Bristol, 2016
36. Rashid AR, Investigation of through-thickness assembly stresses in composite wings spars, PhD thesis, University of Bristol, 2007
37. Mahmoudi AH, Hossain S, Truman CE, Smith DJ and Pavier MJ, A new procedure to measure near yield residual stresses using the deep hole drilling technique, *Experimental Mechanics*, 49, 595-604, 2009
38. Wijskamp S, Akkerman R and Lamers EAD, Residual stresses in non-symmetrical carbon/epoxy laminates, in Martin MJ and Hahn HT (Eds.), *Proceedings of the 14th International conference on Composite Materials, ICCM14 San Diego, USA*, 2003

## FIGURES

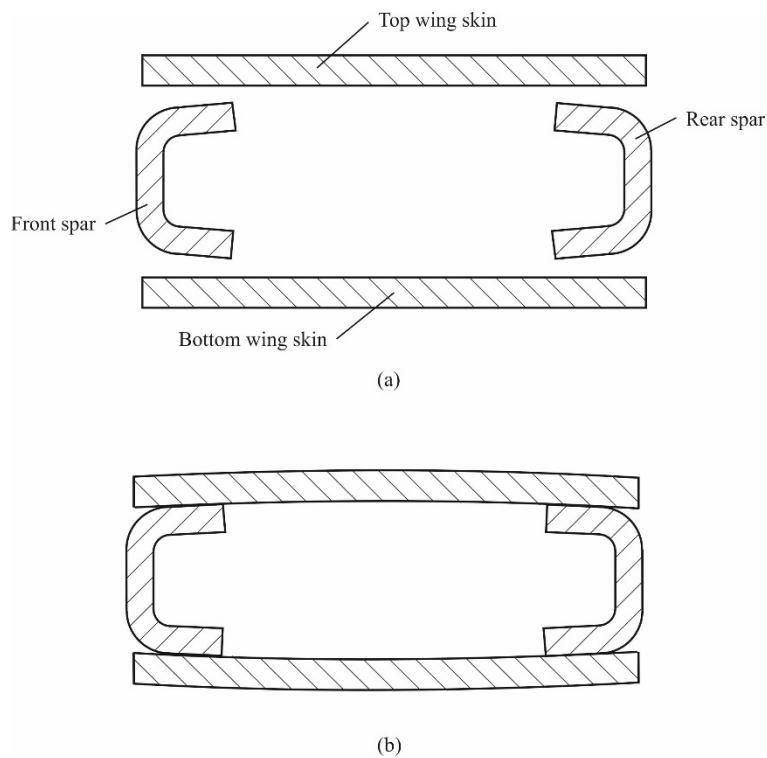


Figure 1 Diagram showing an example of the generation of assembly stress: (a) wing box components before assembly, (b) wing box structure after assembly.

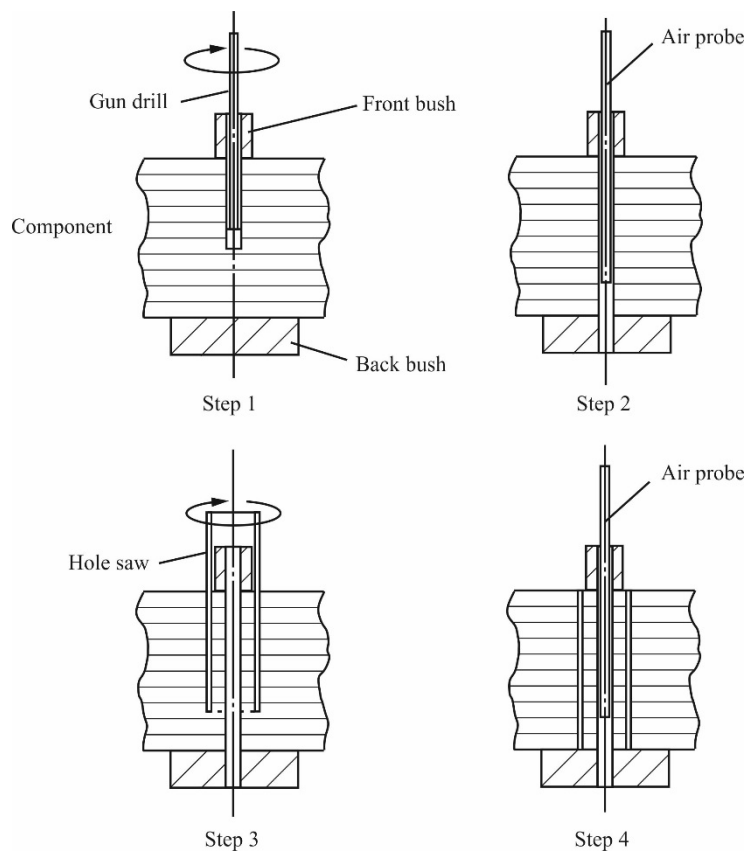


Figure 2 Diagram of the steps used for the deep-hole-drilling method.

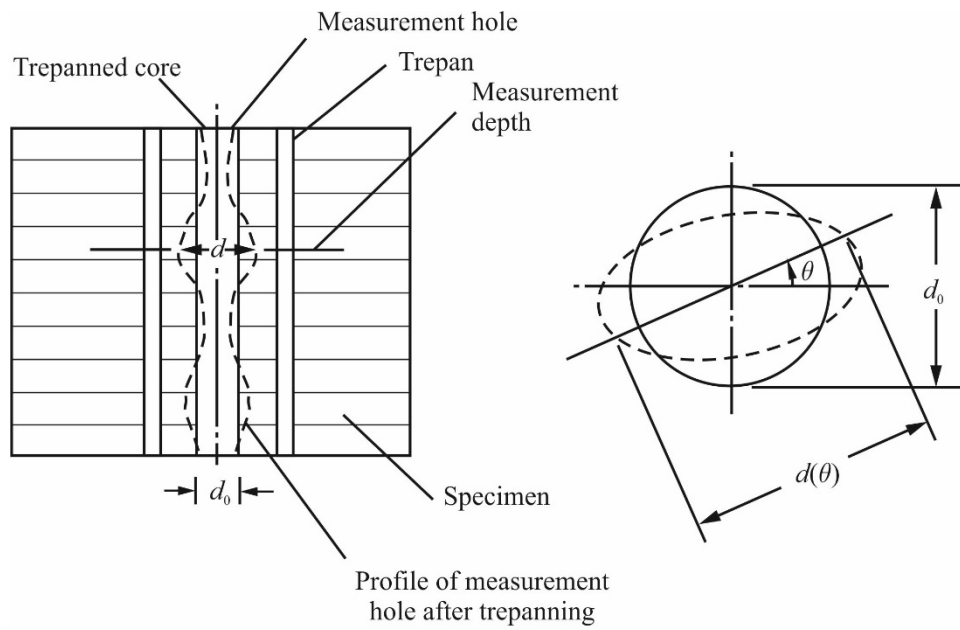


Figure 3 (a) (b)  
Hole distortion measured by the deep-hole-drilling method: (a) cross section showing hole distortion with depth and (b) hole distortion at one example depth.

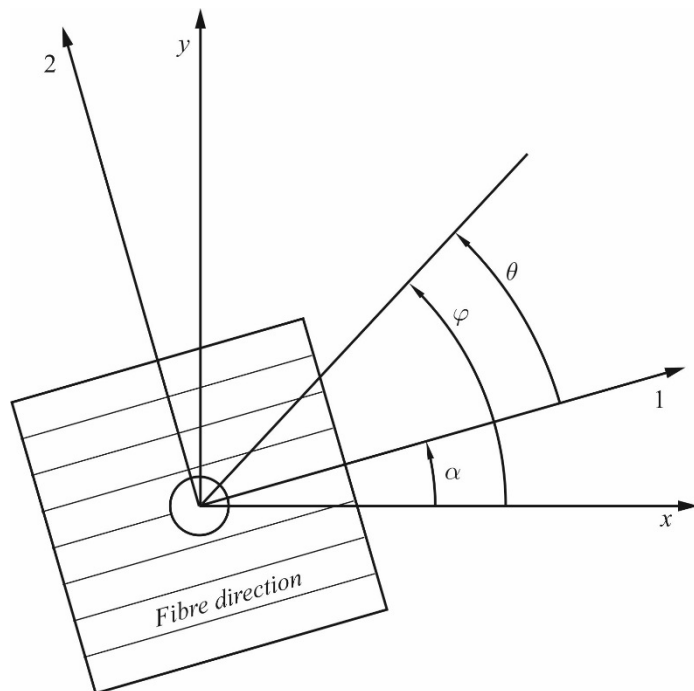


Figure 4 Unidirectional laminate showing the relationship between the fibre direction ( $\alpha$ ) and measurement ( $\theta$ ) angles in reference to the global axes.



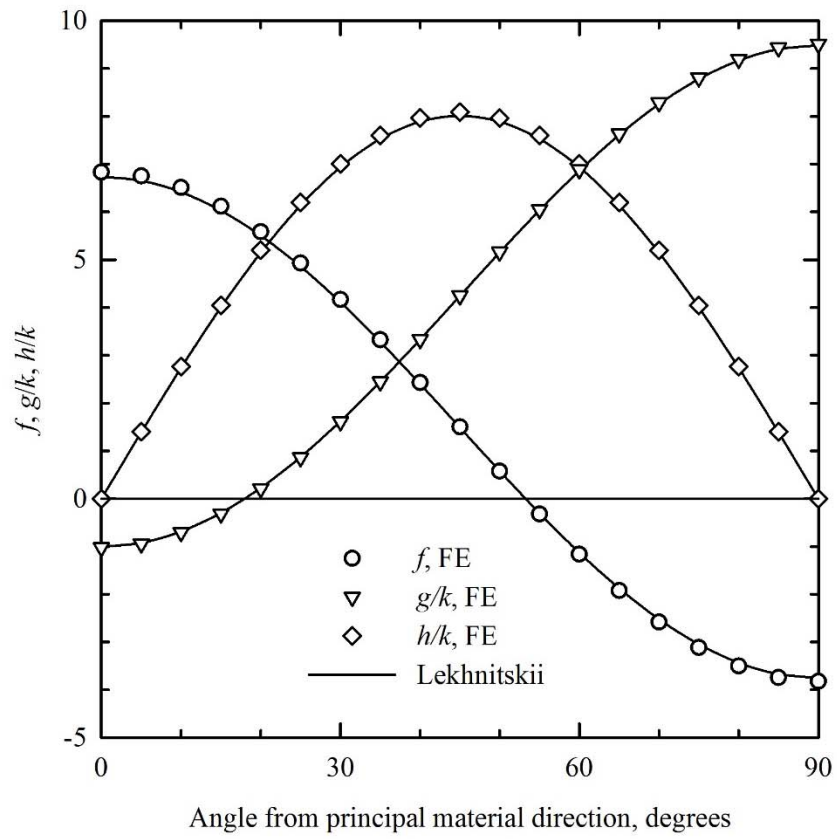


Figure 5 Comparison of the DHD coefficients evaluated by Lekhnitskii's method with FEA.

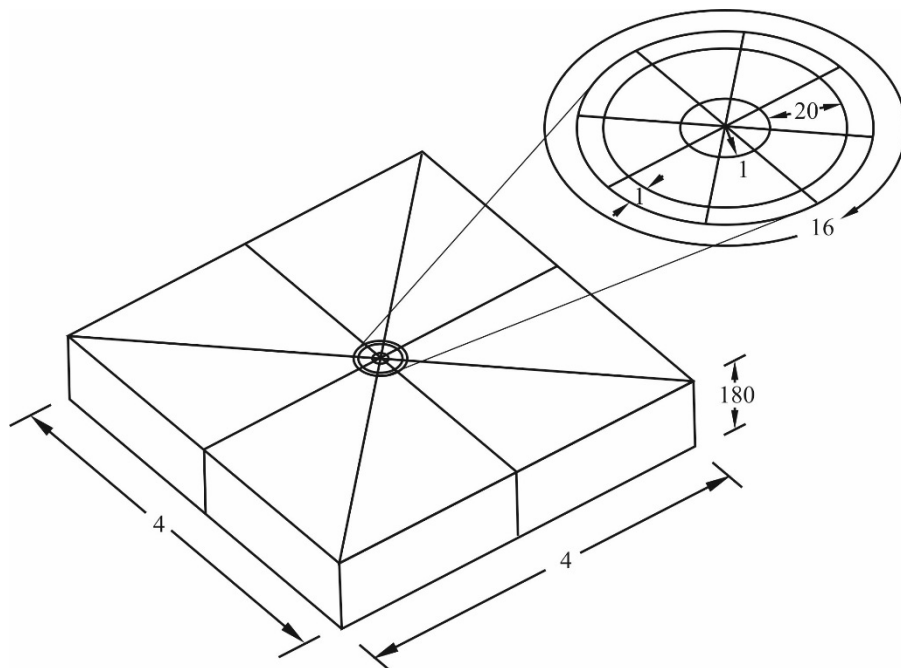


Figure 6 FE mesh used for the simulation of the cure stress measurement.

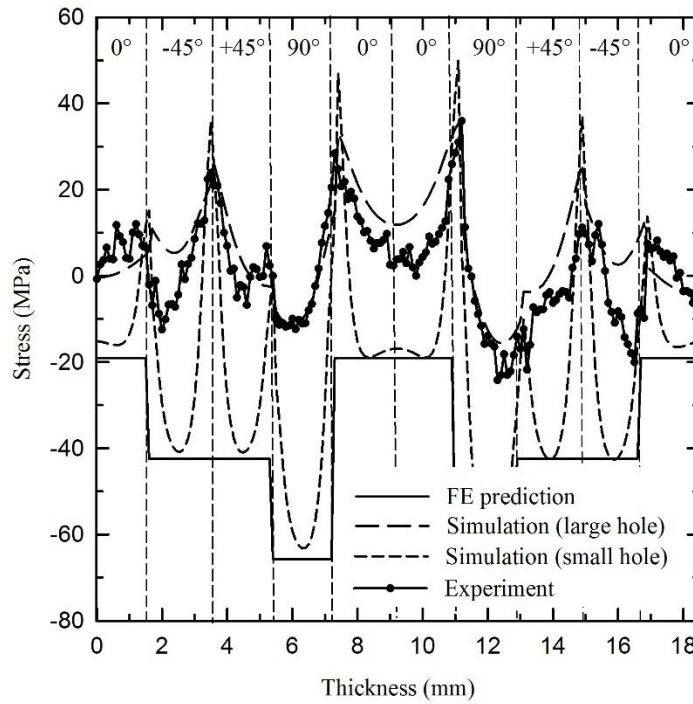


Figure 7 Comparison of cure stress predicted by FEA, simulated by FEA for two different hole sizes and experiment.

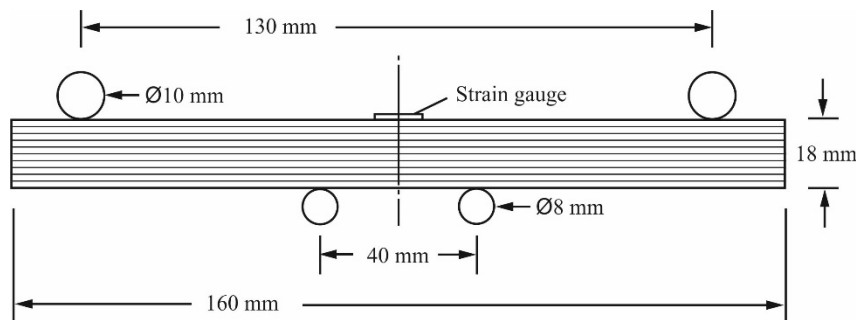


Figure 8 Dimensions of the composite specimen used to measure in-plane assembly stress.

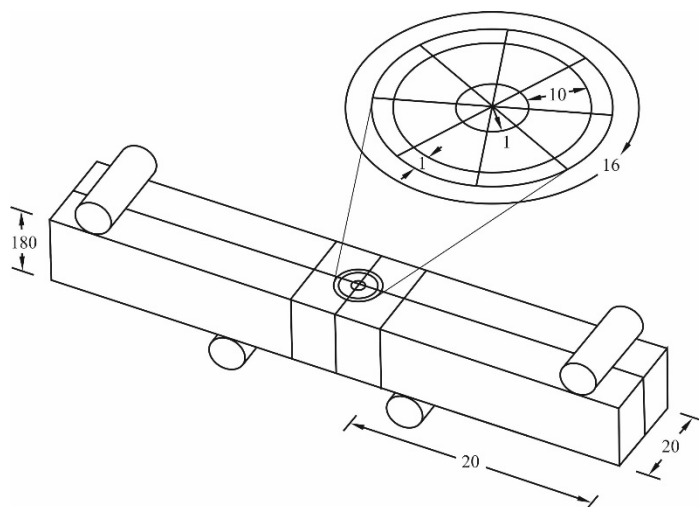


Figure 9 FE mesh used for the simulation of the in-plane assembly stress measurement.

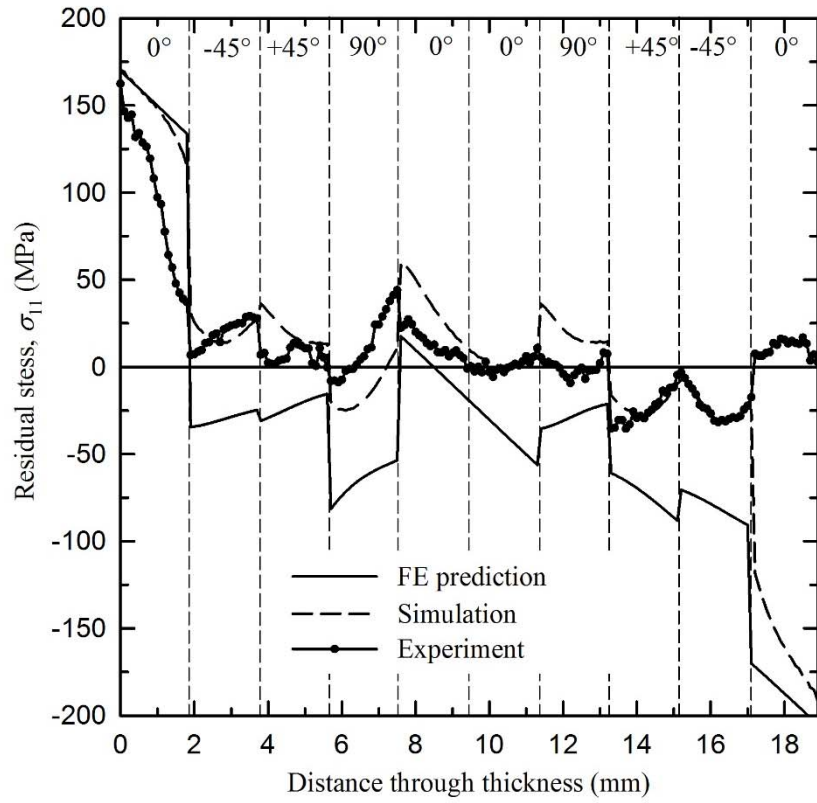


Figure 10 Comparison of the in-plane assembly stress predicted by FEA, simulated by FEA and measurement.

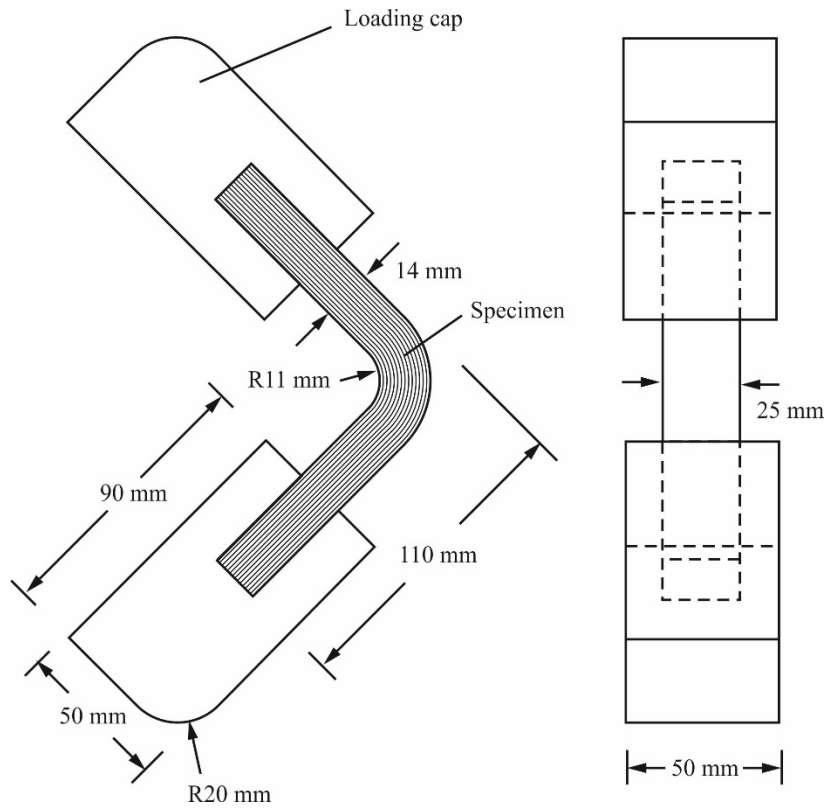


Figure 11 Dimensions of the composite angle specimen used to measure through-thickness assembly stress.

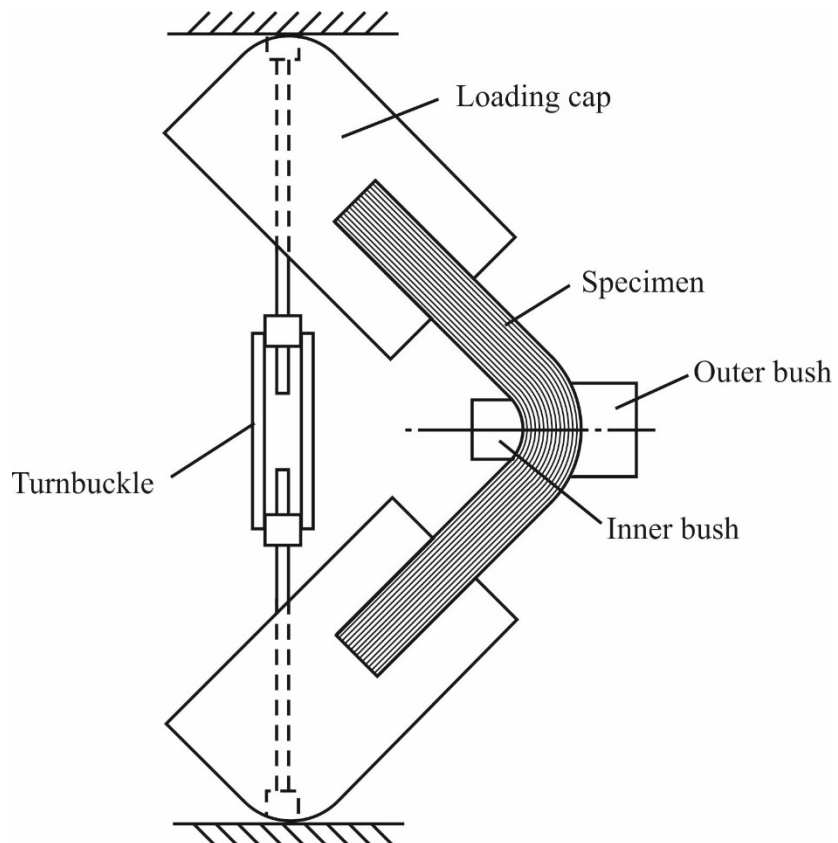


Figure 12 Diagram showing the method used to pre-load the composite angle specimen.

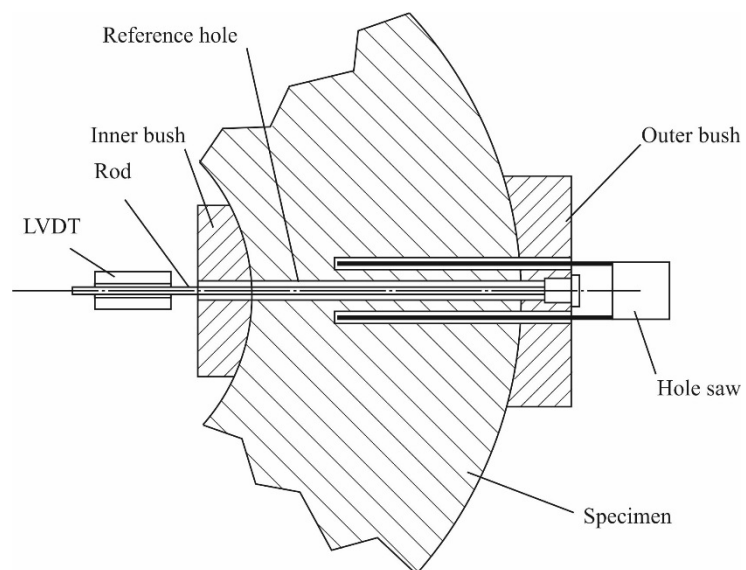


Figure 13 Diagram showing the method used to measure through-thickness assembly stress.

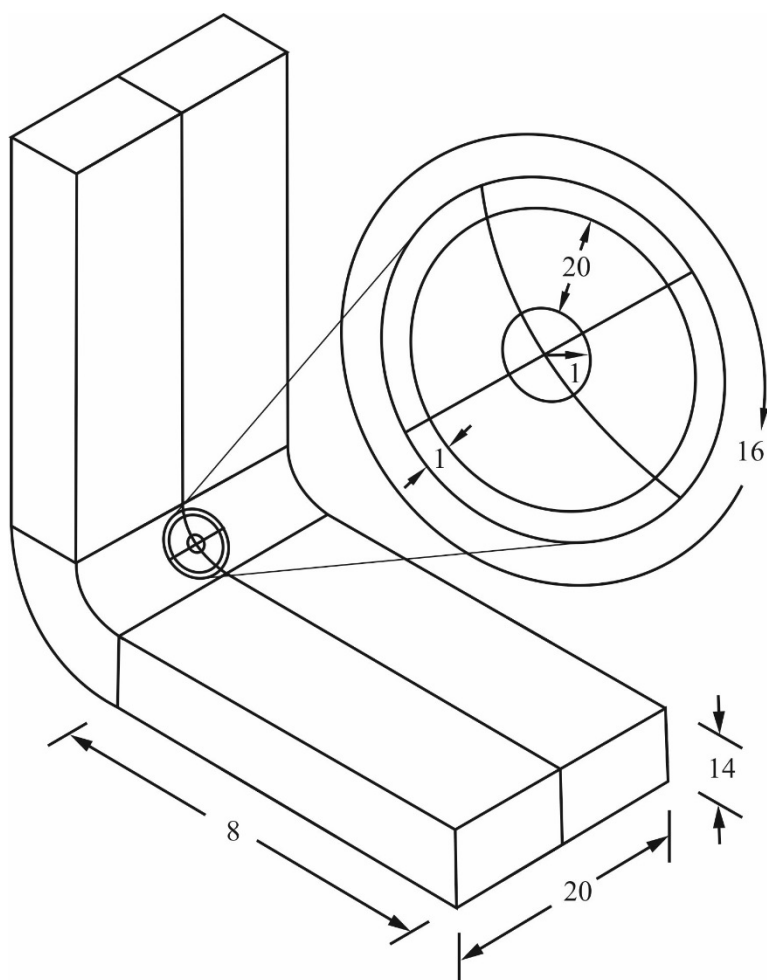


Figure 14 FE mesh used for the simulation of through-thickness assembly stress.

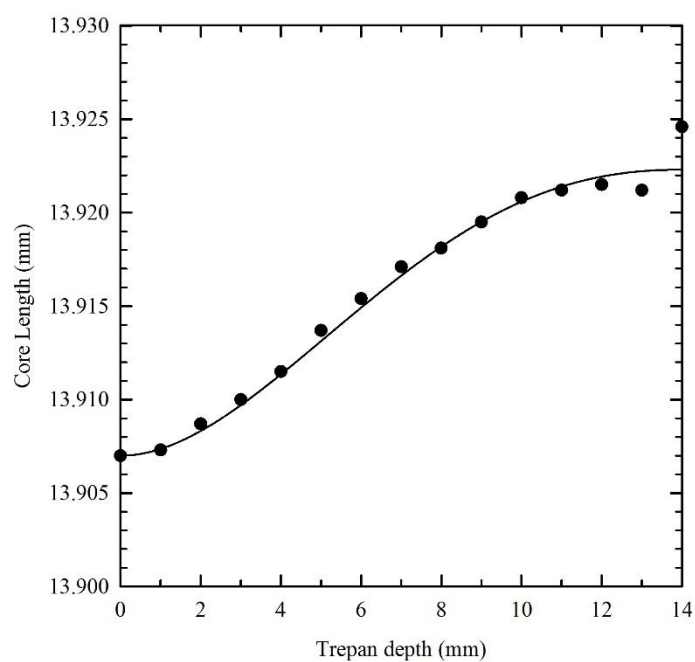


Figure 15 FE simulated measurement of the change in length of the core with trepan depth.

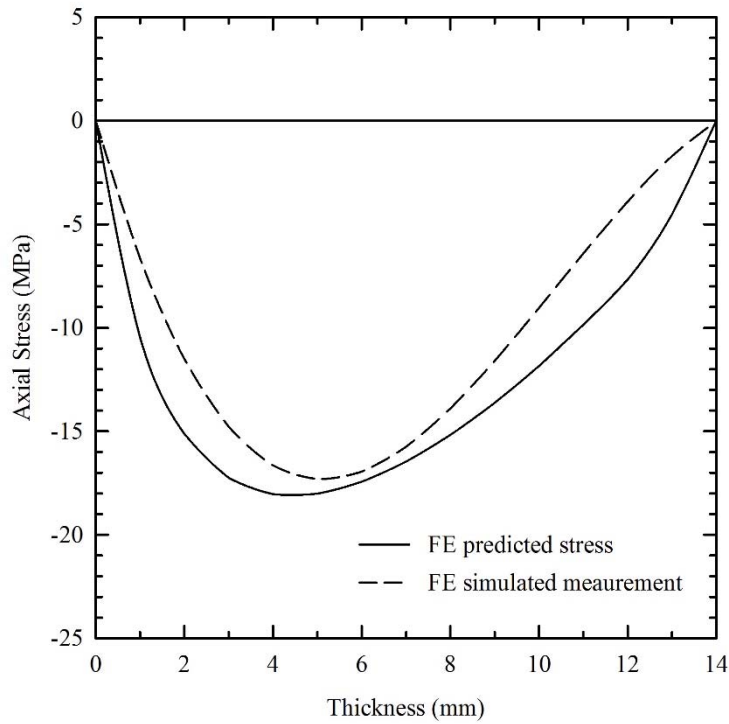


Figure 16 Comparison of the through-thickness assembly stress predicted by FEA and simulated by FEA.

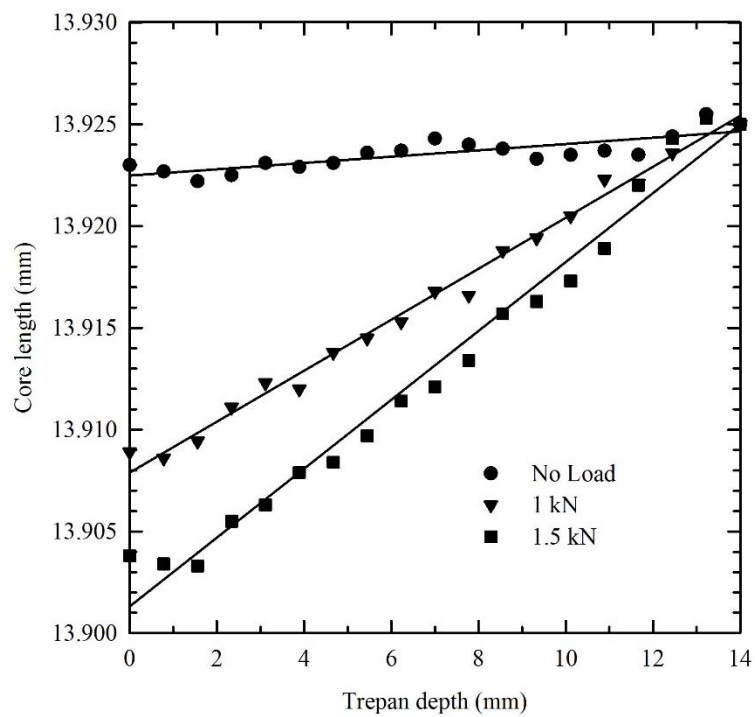


Figure 17 Experimental measurement of the change in length of the core with trepan depth.

## TABLES

Engineering constant	Description	Value
$E_1$	Young's modulus	135 GPa
$E_2$	Young's modulus	9.6 GPa
$E_3$	Young's modulus	9.6 GPa
$\nu_{12}$	Poisson's ratio	0.3
$\nu_{13}$	Poisson's ratio	0.3
$\nu_{23}$	Poisson's ratio	0.435
$G_{12}$	Shear modulus	5.2 GPa
$G_{13}$	Shear modulus	5.2 GPa
$G_{23}$	Shear modulus	3.4 GPa
$\alpha_1$	Coefficient of thermal expansion	$2.8 \times 10^{-7} \text{ }^\circ\text{C}^{-1}$
$\alpha_2$	Coefficient of thermal expansion	$2.8 \times 10^{-5} \text{ }^\circ\text{C}^{-1}$

Table 1 Mechanical and thermal properties of AS4/8552 [38].

Load (kN)	Through-thickness stress (MPa)		
	Experiment	FE prediction	FE simulation
0	-1.8	0	0
1	-10.8	-12.0	-11.5
1.5	-14.5	-18.0	-17.3

Table 2 Comparison of experimentally measured with FE predicted and simulated through-thickness stress.